3.A; 4E *Nuclear Physics* **29** (1962) 33—65; © *North-Holland Publishing Co., Amsterdam*

DECAY OF Sm^{153} TO Eu^{153}

T. SUTER †, P. REYES-SUTER †, S. GUSTAFSSON and I. MARKLUND ††
Institute of Physics, Uppsala, Sweden

Received 27 July 1961

Abstract: The decay of Sm^{153} to Eu^{153} has been investigated by means of an iron yoke double focusing spectrometer, gamma-gamma and electron-gamma coincidence spectrometers. A precision measurement of the 69.672 keV line has been performed with an iron-free double focusing spectrometer. Internal conversion lines and photo-electric lines of the following transitions have been measured and their energies determined with a precision of a few parts in 10^4: 69.672; 75.34; 83.37; 89.47; 97.45; 103.174; ≈ 104.8; 172.85 keV. Conversion electron and gamma intensities, multipolarities, mixing ratios and conversion coefficients are given. Using the photo-electron method, 16 other weak transitions were measured with a resolution of 0.5 % to 0.25 %: 151.5; 411.5; 424.3; 437.7; 449.7; 463.6; 521.3; 531.4; 533.2; 539.1; 555.2; 578.6; 596.9; 603.1; 609.1; 636.0 keV. Difficulties in the computation of intensities of low energy gamma rays from external conversion measurements are briefly discussed. A decay scheme is proposed on the basis of the energy data and a quantitative analysis of the gamma-gamma and electron-gamma coincidences. Excited levels at the following energies have been established: 83.37; 97.45; 103.17; 172.85; (191.4); 634.6; 636.4; (694.3); (706.4) keV.

1. Introduction

It is well known that nuclei in the mass region $150 < A < 190$ have a non-spherical equilibrium shape. The properties of such nuclei, of both even and odd mass, are predicted and explained with high accuracy by the unified model. The neighbouring nuclei outside the above mentioned region are not as well understood. A study of the excited levels of the odd-proton nucleus $_{63}Eu^{153}_{90}$ is therefore of special interest because of its position just on the edge of strongly deformed nuclei.

Sm^{153} (47 h) and Gd^{153} (225 d) both decay to Eu^{153}, but as the Q-value of the Sm^{153} decay is larger, about 800 keV compared to about 200 keV for Gd^{153}, it allows higher excited states to be studied. A great number of investigations [1]) have been published on the Eu^{153} levels excited in the Sm^{153} or Gd^{153} decay or in Coulomb excitation. Based on these investigations Mottelson and Nilsson [2]) have given the decay scheme reproduced in fig. 1 and interpreted it in terms of the unified model. A ground state spin $I = \frac{3}{2}$ for Sm^{153} was measured by Cabezas *et al.*[3]) using the atomic beam resonance method. The spin of the Eu^{153} ground state has also been directly measured [4, 5]), its value being $I = \frac{5}{2}$.

Studies of the beta spectrum from Sm^{153} have shown [1]) the presence of three main components with the maximum energies listed in table 1.

† On leave from the Comisión Nacional de Energía Atómica, Buenos Aires, Argentina.
†† Present address: Institute of Physics, Chalmers University of Technology, Gothenburg V, Sweden.

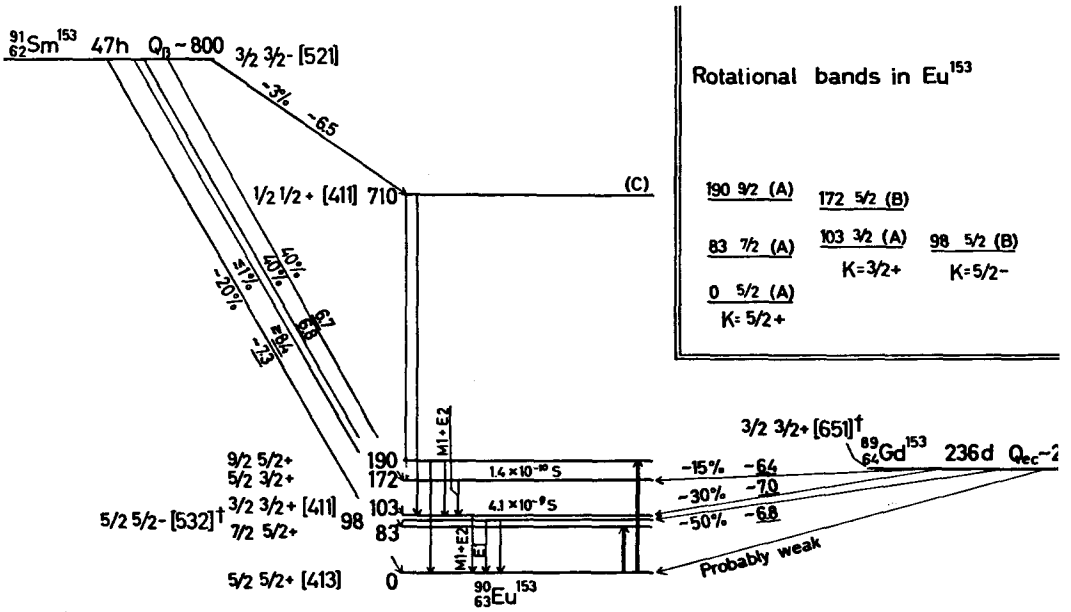

Fig. 1. Decay scheme according to Mottelson and Nilsson [2]). The cross (†) denotes states associated with a smaller nuclear deformation.

TABLE 1

Reported beta branches from Sm^{153}

Graham and Walker [39])		Dubey *et al.* [6])		N. Marty [18])	
Max. energy (keV)	Intensity (%)	Max. energy (keV)	Intensity (%)	Max. energy (keV)	Intensity (%)
810±10	20	825±10	22	820±10	22
710±15	50	720±10	38	720±15	35
640±15	30	645±10	40	650±15	43

TABLE 2

Precision transition energy determinations

Authors	Instrument	E_γ (keV)	
		103.2	69.7
Beckman [7])	Bent crystal spectrograph	103.18 ±0.04	69.66 ±0.02
Bergvall [8])	Bent crystal spectrometer	103.175±0.004	
Walters *et al.* [9])	Bent crystal spectrograph	103.17 ±0.04	69.66 ±0.02
Present work	Iron-free double-focusing spectrometer		69.672±0.006

Gamma rays of 70, 100, 170, 530 and 600 keV from the Sm^{153} decay have been observed with gamma scintillation spectrometers [6, 34, 36]). Bent crystal spectrometer measurements have been reported for the 70, 97 and 103 keV lines [7–9]) (table 2). Conversion electrons corresponding to gamma rays of energies 69, 84 and 103 keV have been reported by Marty [10]). No internal conversion lines of gamma rays above 103 keV have been observed up till now, with the exception of a 548 keV line reported by Lee and Katz [11]).

The Coulomb excitation experiments [1, 19]) on Eu^{153} show the existence of two levels at 83 keV and 190 keV belonging to the ground state rotational band.

During the present investigations several articles have appeared on the low excited levels of Eu^{153}. The most accurate data were obtained by Graham *et al.*[12]) who studied the decay of Gd^{153} with the Chalk River iron-free double focusing spectrometer. They found conversion lines corresponding to the following gamma energies (keV): 14.09; 19.82; 69.67; 75.43; 83.37; 89.47; 97.47; 103.2; 172.88. Recently Moussa and Monnand [13]) found that weak conversion lines corresponding to gamma rays of 19.8 keV and 97 keV also were present in the Sm^{153} decay. The data available for the high energy levels in Eu^{153} are rather contradictory. Lee and Katz [11]) found that the 548 keV transition goes to the ground state. Marty [10]), instead, proposed that a 545 keV gamma ray goes to the 103 keV level. Finally Dubey *et al.*[6]) concluded from their coincidence measurements that this transition had to be placed between a 700 keV level and the 172 keV level. In their decay scheme, which has been the one generally adopted, a 600 keV gamma ray goes from the 700 keV level to the 103 keV level as in fig. 1.

Mottelson and Nilsson suggested in their review article [2]) that the weakly fed 700 keV level was a single-particle level with the Nilsson quantum numbers $\frac{1}{2}+[411]$. In such a case there should exist two close lying levels at about 700 keV with spins $I = \frac{1}{2}$ and $I = \frac{3}{2}$, the second one being a member of the rotational band based on the single-particle level $\frac{1}{2}+[411]$. These levels were suggested to decay mainly to the 173 and 103 keV levels giving two double lines around 530 and 600 keV respectively.

The aim of the present investigation was to confirm these ideas on the high energy levels. However, the initial experiments showed that the high energy spectrum had a more complex structure than the suggested one. We then decided to undertake a complete study of this decay and to look for possible beta and gamma vibrational levels similar to those recently observed in neighbouring even nuclei [38]).

2. Internal Conversion

2.1. SOURCE PREPARATION

The sources were produced by neutron irradiation of isotopically enriched Sm_2O_3. The material used in the preliminary runs had a quoted atomic percentage

abundance of (89.9±0.1)% Sm^{152}. No other half-lives than that corresponding to Sm^{153}, were observed during the internal conversion experiments. The photo-conversion measurements, however, showed a small contribution of the 9 h activity of Eu^{152m} at the beginning of the runs. In the later experiments we therefore only used material with an atomic percentage of (99.06±0.05)% of Sm^{152}. In addition the amount of Eu present in the material was reduced from 0.6 % to < 0.02 %. Some of the irradiations were performed in the Stockholm reactor in a neutron flux of about 2×10^{12} neutrons $(cm^2.s)^{-1}$. To increase the specific activity for detection of some weak low energy lines, a sample was irradiated in the Risø reactor (Roskilde, Denmark) in a flux of 5×10^{13} neutrons $(cm^2.s)^{-1}$. To prepare the internal conversion sources, hydrochloric acid was added to the irradiated Sm_2O_3. After drying, the material was redissolved with a drop of water to enable the filling of a crucible. The deposition was performed by evaporation in vacuum onto 2 mg/cm² aluminium strips.

2.2. MEASUREMENTS WITH AN IRON-FREE DOUBLE FOCUSING SPECTROMETER

An iron-free double focusing beta spectrometer [16] ($\rho_0 = 30$ cm, $\beta = \frac{3}{8}$) was employed to give a precise determination of the energy and intensity of the 69.67 keV transition by measuring its K conversion electron momentum relative to the K conversion line of the 103.175 keV transition of which the energy is known from precise crystal spectrometer measurements (table 2). The $B\rho$ values obtained from three different runs using different methods to determine the peak position did agree within 1 : 10 000. The gamma energy was found to be

$$E_\gamma = 69.672\pm0.006 \text{ keV}.$$

The energies of the K and L conversion lines were then computed using the accurate binding energies given in ref. [17]). The adopted values used for calibration in the later experiments are summarized in table 3. The following intensity

TABLE 3

Calibration data used

E_γ (keV)	Shell	E_e (keV)	$B\rho$ (G . cm)
103.175±0.004	K	54.652±0.004	809.12±0.03
	L_I	95.118±0.004	1087.31±0.02
	L_{II}	95.553±0.004	1090.00±0.02
	L_{III}	96.193±0.004	1093.96±0.02
69.672±0.006	K	21.149±0.006	495.44±0.06
	L_I	61.616±0.006	861.90±0.05
	L_{II}	62.050±0.006	865.10±0.05
	L_{III}	62.690±0.006	869.81±0.05

ratio was obtained:

$$I(\text{K } 69.7) : I(\text{K } 103) = 0.538 \pm 0.020.$$

Since Geiger tubes with a cut-off estimated to be 3.5 keV were used, no window absorption correction was necessary.

Very few electron intensity data have been published up till now. Moussa and Monnand[13]) give only the ratio of the total electron intensities of the 70 and the 103 keV transitions. Their result $I_e(70) : I_e(103) = 0.70 \pm 0.02$ is in disagreement with our value of 0.55 ± 0.02, obtained by using also the K/(L+M+N) ratios from our results in the next paragraph. The specific activity of our source was more than 20 times higher than that quoted in ref. [13]).

2.3. MEASUREMENTS WITH AN IRON-YOKE DOUBLE FOCUSING SPECTROMETER

A double focusing iron-yoke spectrometer ($\rho_0 = 50$ cm, $\beta = \frac{3}{8}$) similar to that described by Hedgran *et al.*[14]) was used for both the internal and the external conversion experiments. The magnetic field was continuously measured against the field of an iron-free Helmholtz coil using a pair of synchronously

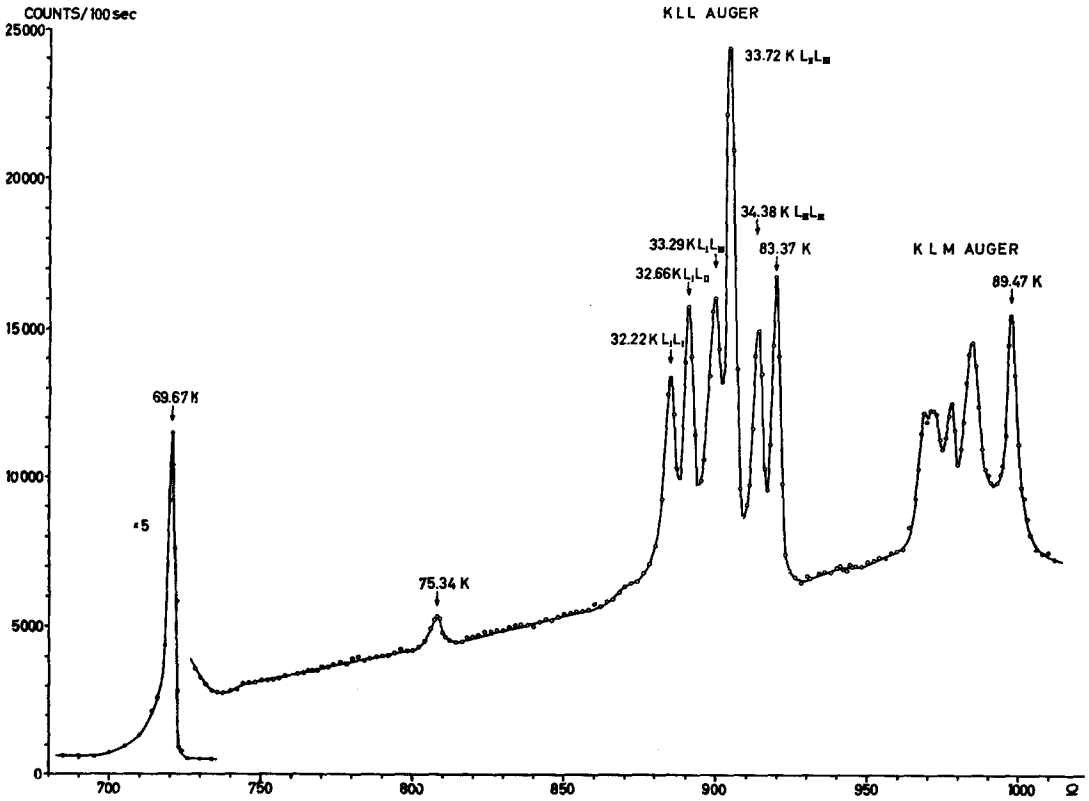

Fig. 2a. Internal conversion spectrum. The parts of the spectrum drawn in full circles or with crosses have been measured with better resolution.

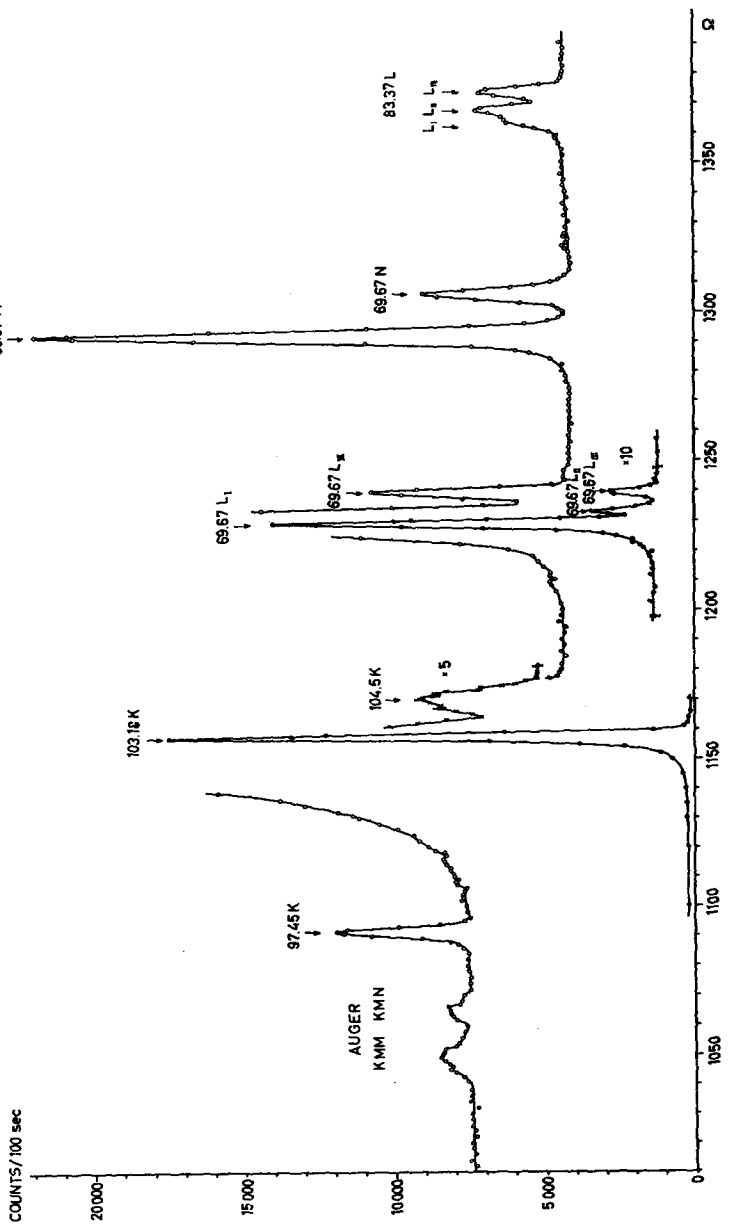

Fig. 2b. See caption fig. 2a.

rotating coils [15]). Earlier experiments performed with this spectrometer have shown that relative measurements of electron momenta can be performed with an accuracy of the order of $(1–2) \times 10^{-4}$. The sources had an area of 2×20 mm. The spectrometer baffles were usually set to obtain a resolution of 2 $^0/_{00}$ (when no energy loss is present), the transmission was then about 1.5 $^0/_{00}$. The cut-off energy of the Geiger-Müller window was about 15 keV.

The internal conversion spectrum obtained with this spectrometer is shown in figs. 2a, 2b, 2c. The measurements covered the electron energy region from 20 to 155 keV. The resulting energies and intensities are given in table 4a

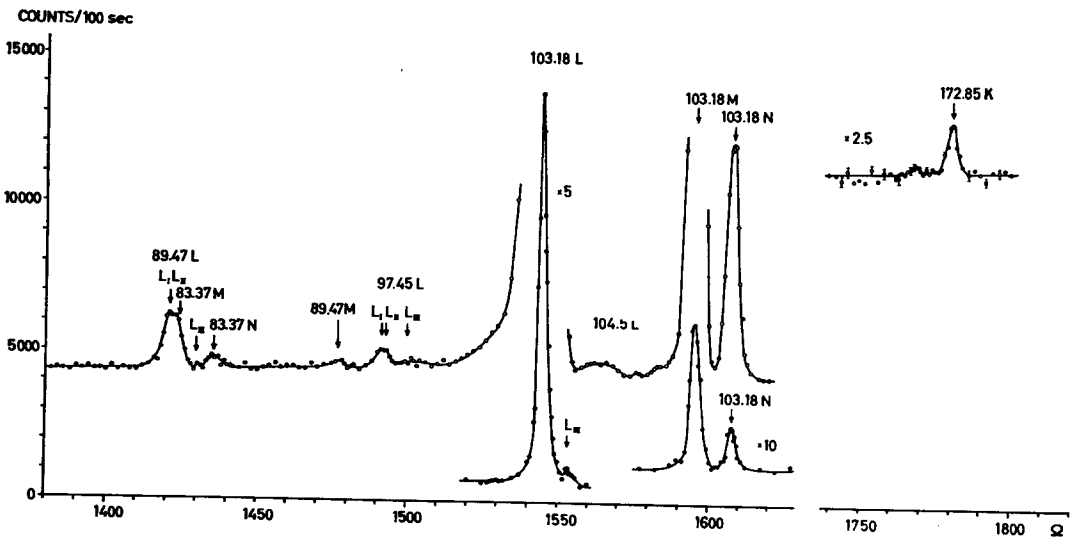

Fig. 2c. See caption fig. 2a.

and 4b. The rate of decay of all the lines reported in table 4a was found to be the same within ± 15 %. The intensities were corrected for absorption in the Geiger-Müller window, but this correction was only a few percent, except for the K 75 and the K 69.7 lines. However, since the intensity of the K 69.7 line was known from the measurements with the iron-free double focusing spectrometer the corrected K 75 intensity was easily determined. The intensity of the weakest lines that easily could be identified on the continuous spectrum was 1 to 2 parts in 10^{-4} of the intensity of the K 103.2 line.

Our internal conversion results are given in table 4a and 4b. The energy determinations obtained in the present measurements are in very good agreement with those reported for Gd^{153} by Graham *et al.* [12]).

Accurate conversion intensities, K/L and L subshell ratios of most of the transitions are determined. See tables 4, 5 and 6. From our ratios we have computed the multipolarities and the mixing ratios using Sliv's tables [18]).

TABLE 4a

Internal conversion results

Adopted transition energy (keV)	Electron energy (keV)	Conversion shell	Transition energy calculated from conv. line (keV)	Relative electron intensity	Relative total conversion intensity
69.672±0.006 [a])	21.18±0.02	K	69.70	5380±200 [a])	6700
	61.66±0.015	L_I	69.71	792±40	
	62.09±0.02	L_{II}	69.71	116±10	
	62.72±0.02	L_{III}	69.70	73±7	
	67.9±0.1	M	69.7	223±10	
	69.35±0.1	N	69.7	59±4	
75.34±0.05	26.83±0.05	K	75.34	18±2	
83.37±0.02	34.87±0.02	K	83.37	147±5	250
	75.35±0.04	L_I	83.40	22±5	
	75.77±0.03	L_{II}	83.39	31±3	
	76.41±0.03	L_{III}	83.39	31±3	
89.47±0.04	41.00±0.04	K	89.47	120±10 [b])	160
	81.43±0.07	L_I	89.49	35±3 [c])	
	81.80±0.10	L_{II}	89.42		
	82.46±0.07	L_{III}	89.44	≈ 1	
97.45±0.04	48.93±0.04	K	97.45	50 ±2	60
	89.37±0.1	L_I+L_{II}	97.43	7.7±1.5	
	90.45±0.15	L_{III}	97.43	≈ 1	
103.175±0.004 [d])	54.65±0.015	K	103.17	10 000±300	12 300
	95.14±0.02	L_I	103.19	1600±50	
	95.57±0.04	L_{II}	103.19		
	96.21±0.03	L_{III}	103.19	53±15	
	101.38±0.05	M	103.2	533±100	
	102.87±0.05	N	103.2	97±7	
172.847±0.010	124.30±0.06	K	172.82	6.3±0.5	

[a]) Data obtained from our iron-free double-focusing spectrometer measurements.
[b]) Not resolved from KLN Auger lines.
[c]) Not resolved from M 83.4 keV line.
[d]) Calibration line from ref. [8]).

Very few intensity ratios have been reported up till now. In addition to the already mentioned $N_e(69.7) : N_e(103.2)$ ratio given by Moussa and Monnand only K/L ratios of the two strongest transitions have been given. These intensity ratios are listed in table 6.

We have also observed some weak transitions reported in table 4b. Those found at 59.6 keV and 100.0 keV might already ratios have been conversion lines of a 108.0 keV transition. Conversion mentioned strongest

to a similar transition energy have been reported in several Coulomb excitation experiments [19, 20]). Bernstein and Graetzer [19]) give a gamma transition energy of 109 keV (no error quoted) and a K/L ratio of 3.4. The data obtained by

TABLE 4b

Internal conversion results (probable assignments)

Electron energy (keV)	Probable conversion shell	Proposed transition energy (keV)	Relative electron intensity
30.8 ± 0.2	K(?) or L(?)	79.4 ≈ 38.9	2 ±1
55.80± 0.06	K	104.33	16 ±4
56.04± 0.05	K	104.57	24 ±4
56.23± 0.07	K	104.75	21 ±4
56.39± 0.07	K	104.91	11 ±4
97.3 −97.9	L_{III}	104.3 −104.9	7 ±3
59.6 ± 0.2	K	108.0	3 ±1.5
100.0 ± 0.2	L_I	108.0	1.5±0.5
122.7 ± 0.1	K	171.2	1 ±0.5

TABLE 5

Multipolarities and mixing ratios

E_γ (keV)	$\frac{L_I}{L_{II}}$	$\frac{L_I}{L_{III}}$	$\frac{L_I+L_{II}}{L_{III}}$	Multipole assignment	δ^2
69.7	6.8	10.9	12.4	98.4 % M1+1.6 % E2	0.0160±0.0020
75.3				(E1) [a])	
83.4	0.72	0.72	1.72	64 % M1+36 % E2	0.56 ±0.20
89.4				M1+E2 [a])	
97.5			4	(E1) [a])	
103.2			30	98.9 % M1+1.1 % E2	0.011 ±0.003

[a]) From α_K and K/L.

TABLE 6

K/L ratios

E_γ (keV)	Lee and Katz [11])	Marty [10])	Graham and Walker [29])	Moussa and Monnand [13])	Bernstein and Lewis [44]) [a])	Present work	Theoretical [b])
69.7	3.8	>4.4	4.6	7.2		5.5	6
83.4					1.7	1.8	2.2
89.4						3.5 [c])	M1 7.5
							E2 0.9
97.5						6	6.7
103.2	6.2	6.2	6	7.0		6.1	6.6

[a]) Coulomb excitation.
[b]) Obtained assuming the multipolarities and mixing ratios given in table 5.
[c]) See footnotes [b]) and [c]) of table 4a.

Class and Meyer-Berkhout [20]) are 107 ± 2 keV and K/L = 2.2. These agree with the values we have obtained. This transition goes from the 190 keV level to the 83 keV level. If our 108.0 keV transition is identical with the above mentioned one, the energy of the 190 keV level would be 191.4 ± 0.2 keV. According to Bernstein and Graetzer the intensity of the K 190 conversion line relative to the L conversion line of the 109 keV transition is 0.92 ± 0.05 and this is about the lowest intensity that we could distinguish above the background. This accounts for the fact that the 191.4 keV transition was not observed in our experiments.

A group of weak conversion lines is found at an electron energy of 56 keV. This group is composed of at least three lines. In table 4b we report a decomposition into four lines. Since we have seen a group of lines in the external conversion experiments at an energy corresponding to 105 keV, we assume in table 4b that these lines are K conversion lines of gamma rays of energies of 104.3 to 104.9 keV. However, we cannot exclude the possibility of the existence of L conversion lines in this group corresponding to a transition of about 64 keV.

Another two weak lines appear at electron energies of 30.8 ± 0.2 keV and 122.7 ± 0.1 keV (intensities 2×10^{-4} and 1×10^{-4} of the K 103.2 line). The first one is either a 79.4 keV or a 39 keV gamma transition, the second one is probably a 171.2 keV gamma transition.

The region around K 530 has been measured in internal conversion but no line with an intensity higher than 2 parts in 10^4 could be seen.

The present measurements are in general agreement with the low energy part of the earlier decay scheme shown in fig. 1. (See also fig. 7.) We have found all the lines seen in the Gd^{153} decay, except the conversion lines of the 14 and 19 keV transition, which did not fall in the region of our measurements.

3. Photo Conversion

3.1. SOURCE AND GEOMETRY

The iron yoke double focusing spectrometer was also used to study the external conversion spectra. Several runs were performed with the 89.6 % isotopically enriched samarium oxide. 50 to 70 mg of the oxide were enclosed in a spectroscopically pure aluminium capsule. The inner dimensions of the capsule were 2.0 mm diameter and 20 mm length. The wall thickness was 0.2 mm. The capsule was irradiated in the Stockholm reactor with a flux of $(2 \text{ to } 3) \times 10^{12}$ neutrons $(\text{cm}^2 \cdot \text{s})^{-1}$ for periods of about one week. The sources had activities in the range of 200 to 500 mCur. The aluminium capsule was enclosed in a copper tube with a wall thickness of 0.4 mm to stop the electrons emitted by the source. The mean source-to-converter distance was 1.8 mm. The background measurements showed during the first hours a 9 h

half-life component which was attributed to an Eu^{152m} impurity. The beta spectrum of this isotope has high energy electrons, which were not stopped by our 0.4 mm thick copper absorber. Later on the very pure enriched samarium oxide (99.06 ± 0.05 % Sm^{152}) was used and no 9 h activity could be detected. When this source had decayed more than 9 half-lives, several scintillation spectra were taken, which showed the presence of a very weak long half-life activity (12 y $Eu^{152} + 16$ y Eu^{154}). However, the intensity of the strongest lines of these impurities was computed to be about 1:30 of the weakest line observed in the external conversion spectra, when the measurements started.

Because of the weakness of the high-energy lines it was considered necessary to increase the source strength in the final measurements. In order to avoid too high activities the geometry was also improved. An aluminium capsule of 1.0 mm diameter and 16 mm length (inner dimensions) inserted in a copper tube of wall thickness 0.5 mm was used. The mean source-to-converter distance was reduced to 1.3 mm. In this way it was also possible to make a careful study of the low energy region because of the small correction for source absorption. Rectangular converters, 20 mm high, were used. In most of the experiments the width was 4 mm, but when a resolution better than 0.4 % was required, the converter width was 2 mm. An amount of 10 mg of the highly enriched samarium oxide was irradiated for 65 hours in the Risø reactor with a flux of 9×10^{13} neutrons per $cm^2 \cdot s$. When the measurements started, the activity of the source was about 5 Cur.

3.2. THE GAMMA ENERGY REGION FROM 60 TO 200 keV

The photo conversion method has been very seldom used for gamma energies below 150 keV in nuclear spectroscopical studies. The present investigation shows that the method can with some care be successfully applied to energies well below 100 keV. However, more information on the angular distribution and the cross section of the photo-electric effect in the different shells is needed to obtain more accurate intensity data.

A large number of converter materials (U_2O_3, Pb, Au, Pt, Yb, Sn, Ag) with thickness varying from 0.2 to 2 mg/cm^2 were used. Most of the converters were prepared by evaporating the material in vacuum onto 2 mg/cm^2 aluminium strips. The thickness was determined by weighing. The uranium oxide converters were prepared by the painting technique [21]). Uranium nitrate was dissolved in amylacetate and painted with a brush onto a stainless steel foil of 8.5 mg/cm^2. The foil was put into an oven (600°–700° C) for one or two minutes. This operation was repeated several times brushing each time in a different direction and rubbing the surface with a soft paper after the foil was taken out of the oven. The thickness was determined by weighing.

Below 150 keV the medium-Z converters proved to be more convenient than high-Z ones. With the latter it is necessary to use the L conversion lines

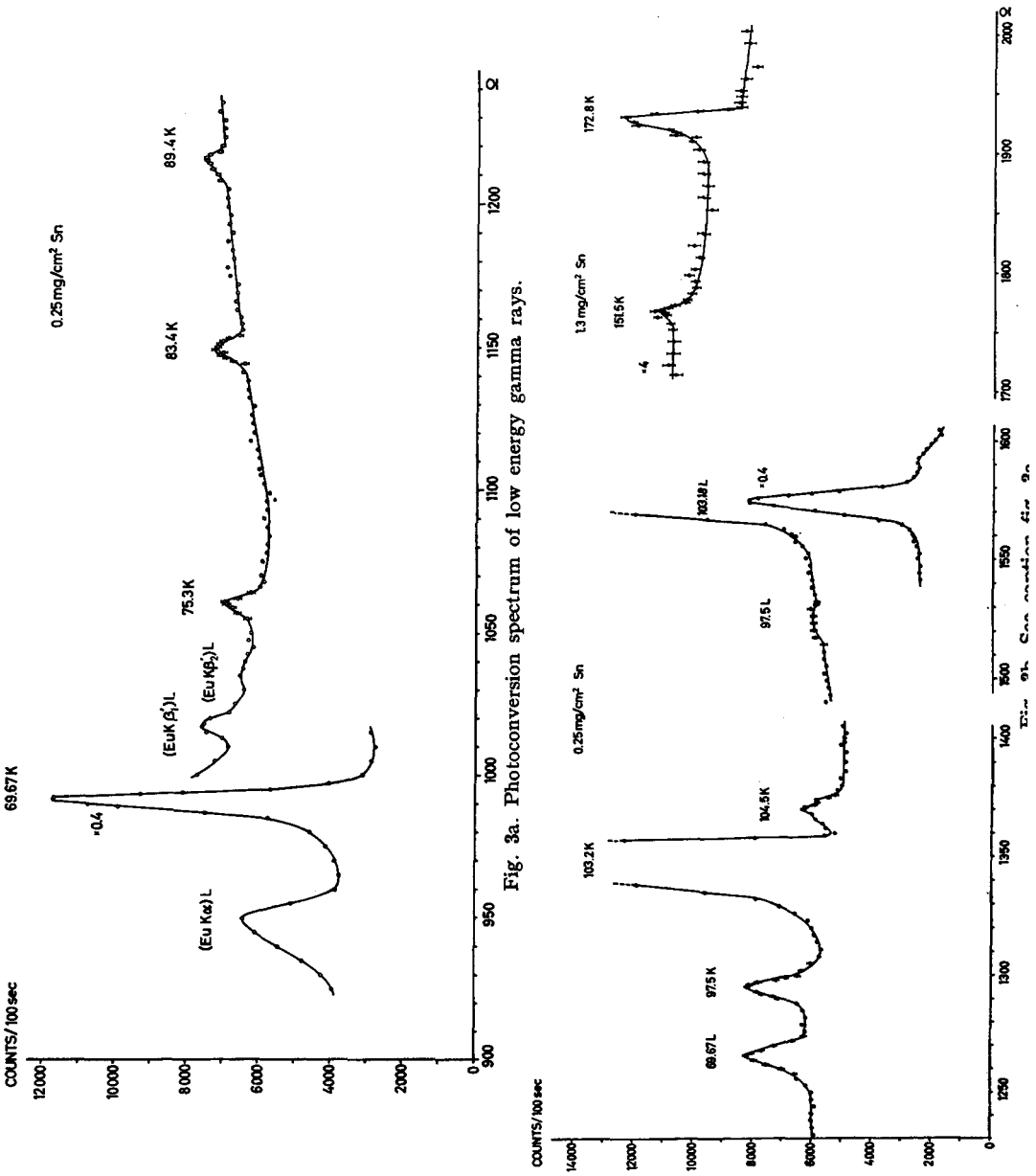

Fig. 3a. Photoconversion spectrum of low energy gamma rays.

and this makes the energy and intensity determinations more difficult. Furthermore the photo-electric cross-section for each L line is one order of magnitude smaller than for the K line. This compensates for the lower photo-electric cross-section of the medium-Z converter. For $E_\gamma < 100$ keV we have about the same values for $\sigma_L(Z = 92)$ and $\sigma_K(Z = 53)$. The best results were obtained with a 0.25 mg/cm² Sn converter. The resolution was 0.7 % for the K 69.7 line and 0.5 % for the K 103 line. The gamma energy region between 150 and 200 keV, where only weak lines were expected, was studied with a 1.3 mg/cm² Sn converter and also with a 2 mg/cm² U_2O_3 converter. The resulting spectra are shown in figs. 3a and 3b and the energies and intensities are collected in tables 7 and 8.

The results obtained with the converters of other materials (particularly the spectra obtained with a 0.3 mg/cm² Yb converter) agree with the presented ones, but less information could be obtained from them.

3.3. INTENSITY DETERMINATION OF LOW ENERGY GAMMA RAYS

The method of Hultberg [22]) is applied to compute the gamma intensities from the external conversion spectra. The gamma intensity is proportional to

$$I_\gamma \propto \frac{A}{f\sigma_K} = \frac{A}{f\sigma_T}\frac{\sigma_T}{\sigma_K},$$

where A is the intensity of the observed K shell photo-electron line and f is the correction factor computed by Hultberg [39]). The f-factor corrects for photo-electric angular distribution, source and converter dimensions and for gamma ray absorption in the source and electron absorber. Rather accurate values for the total photo-electric absorption coefficient $\sigma_T = \sigma_K+\sigma_L+\sigma_M+\ldots$ may be obtained from the tables of G. White Grodstein [23]). However, more precision measurements of the ratios between the cross-section of the different shells are needed. For energies above 300 keV the ratio σ_T/σ_K seems to be fairly constant [22, 24]). In such a case we may drop this factor since we are only concerned with relative intensities. For lower energies, some variation of $\sigma_K/\sigma_T \approx 1-(\sigma_L+\sigma_M)/\sigma_T$ has been reported [24]). Hultberg obtained the following ratios in his external conversion experiments with uranium converters:

$$\sigma_L/\sigma_K = 0.19\pm0.007,\ \sigma_{M'}/\sigma_L = 0.38\pm0.02,\ (\sigma_L+\sigma_{M'})/\sigma_T = 0.20\pm0.006,$$

where $\sigma_{M'} = \sigma_M+\sigma_N+\ldots$. These values were reported to be independent of energy in the energy region 400 to 1300 keV. Some other measurements of these ratios for different energies and Z values are reported [24, 26]), but the information is very scarce for low energies. Grigor'ev and Zolotavin [24]) have recently given the ratios for high-Z material $\sigma_L/\sigma_K \approx 0.18$, $\sigma_M/\sigma_L = 0.29\pm0.04$ and thus $(\sigma_L+\sigma_M)/\sigma_T \approx 0.18$. This last ratio seems to increase to about 0.22 when going down to about 150 keV. Stobbe's [40]) theoretical formulas agree

TABLE 7

Photo conversion results of low energy gamma rays

Adopted transition energy (keV)	E_e (keV)	Conv. shell	Transition energy calculated from external conv. line (keV)	A_γ	$f\sigma$ (b per atom)	Gamma intensity I_γ	Total transition intensity ($I_\gamma(103.2)=10\,000$)
69.672±0.006	40.46±0.03	K	69.67	4 428	130.0	1 920±120	11 500
	65.4	L	≈69.7	410			
75.34 ±0.04	46.17±0.04	K	75.37	125	109.3	65±8	95
83.37 ±0.02	54.21±0.04	K	83.41	105	101.8	58±8	410
89.47 ±0.04	60.34±0.06	K	89.52	75	96.8	43±6	270
97.45 ±0.04	68.32±0.05	K	97.52	330	89.9	207±10	290
	93.2	L	≈97.5				
103.175±0.004	74.05±0.05	K	103.25	15 173	85.6	10 000±300	27 600
	99.0	L	≈103.3	2 360			
	75.8 ±0.3	K	105	170	85.0	115±15	
151.5 ±0.3	122.4 ±0.3[a])	K	151.65	7.8	54.4	8±2[a])	
172.847±0.010	143.57±0.1	K	172.77	25.2	43.5	33±4	≈44

[a]) The K 172.847 line was used as energy calibration and for normalizing the intensity.

TABLE 8

Photo conversion results of high energy gamma rays

Adopted transition energy (keV)	E_e (keV)	Converter	Convers. shell	Transition energy calculated from external conv. line (keV)	Gamma intensity ($I_\gamma(103.2)=10\,000$)
151.5 ±0.3	129.62±0.3	U_3O_8	L_I+L_{II}	≈151	
	133.48±0.3		L_{III}	150.7	
172.847±0.01	151.02±0.3		L_I+L_{II}	≈172.4	
	155.28±0.3		L_{III}	172.45	
	167.2 ±0.6		M	≈172	
411.5 ±0.5	295.93±0.5		K	411.5	1.4±0.3
	392		L_I+L_{II}	≈412	
424.3 ±0.5	308.7 ±0.5		K	424.3	1.3±0.3
437.7 ±1.0	322.1 ±1.0		K	437.7	1.0±0.3
449.7 ±0.7	334.1 ±0.7		K	449.7	1.1±0.3
463.6 ±0.2	348.03±0.2		K	463.63	5.5±0.6
	441.91±0.3		L_I+L_{II}	≈463.6	
521.3 ±0.2	405.75±0.25		K	521.35	2.5±0.3
531.4 ±0.25	415.81±0.25		K	531.41	23 ±2
533.2 ±0.3	417.60±0.30		K	533.20	12 ±1
	510.6		L_I+L_{II}	531−533	
539.1 ±0.3	423.58±0.25		K	539.11	6.2±0.6
555.2 ±0.4	439.6 ±0.4		K	555.2	1.8±0.5
578.6 ±0.4	462.97±0.4		K	578.57	1.0±0.3
596.9 ±0.25	481.35±0.25		K	596.95	4.4±0.5
(598.2 ±0.3)	(482.64±0.30)		K	(598.24)	
603.1 ±0.3	487.46±0.30		K	603.06	1.4±0.2
609.1 ±0.3	493.45±0.30		K	609.05	4.2±0.5
636.0 ±0.5	548.03±0.5	Pb	K	636.04	1.8±0.5

with this increase, but his values are 0.12 at 340 keV and 0.14 at the K edge ($Z = 92$). Finally the absorption measurements [23]) at the K edge in uranium yield the value $(\sigma_L+\sigma_M+\ldots)/\sigma_T = 0.134$. These discrepancies may be explained in part by the fact that the angular distribution was not taken fully into account in all the experiments. However, they do not influence very much the value $\sigma_K/\sigma_T = 1-(\sigma_L+\sigma_M+\ldots)/\sigma_T$, which can be considered as constant to within 7%. For lower Z values, both theory [25]) and experiment [24,26]) agree that σ_L/σ_T decreases with decreasing Z, so that the influence of σ_L/σ_T on σ_K/σ_T becomes still smaller. For silver ($Z = 47$) Grigor'ev and Zolotavin report $(\sigma_L+\sigma_M)/\sigma_T = 0.10$ and they observe a slight increase to about 0.15 for energies near the K edge. Similar values may be expected for tin ($Z = 50$).

The absorption data at the K edge yield for tin $(\sigma_L+\sigma_M+\ldots)/\sigma_T = 0.125$. Hence we may conclude that the variation in σ_K/σ_T with energy is only a few percent for tin.

The factor f in the formula takes into account the angular distribution of the photo-electrons, the absorption of the gamma rays in the source and absorber and the geometry of the source and converter arrangement. We have used Hultberg's formulae and the angular distributions he has given for the photo-electrons produced in uranium converters by gamma rays of 159, 208, 279, 412, 661, 1118 and 1332 keV. It was assumed that the actual cylindrical geometry of source and absorber could be replaced in the computations by a plane geometry. The source was considered to be rectangular with its width equal to its actual diameter. The plane absorbers had the following thickness: (0.4 mm Cu)+(0.2 mm Al). This difference in geometry should not affect the results very much, except for energies below 100 keV where the absorption plays an important role. Coherent scattering was not included in the absorption, since elastically scattered gamma rays may produce conversion electrons that contribute to the photopeak. Since the difference in the absorption coefficient with and without coherent scattering is less than 10 %, its contribution was considered negligible.

Still another fact has to be taken into consideration when converters other than uranium are used. It is assumed that the angular distribution of the photo-electrons is dependent on the photo-electron energy, but not on the Z value of the converter material. The theoretical differential cross-section derived by Sauter [27]) is only a function of the velocity v of the electron and of the direction of emission. However, the approximation $Z/(137v\times c^{-1}) \ll 1$ is included in Sauter's formulae. The largest departures from the theoretical distribution should be expected for high-Z elements. Actually the experimental distribution found by Hultberg for uranium differs from the theoretical one, but the departure of the f factor due to this fact is probably not larger than the other systematic errors introduced in the intensity computations in the low energy region. The foregoing assumption means that if we plot f as a

function of the conversion electron energy, we may use the same curve, regardless of the converter material. However, the absorption of the corresponding gamma rays in the absorber is different in each case, since the energy of the gamma ray that produced a photoelectron of a certain energy depends on the binding energy of the converter material. Hence we obtain one f curve for each Z value. This absorption lowers the value of f below 100 keV rather much; at 70 keV, f is reduced by more than a factor 3. The errors in the determination of the absorber dimensions do then have an increasing importance.

The discussion given above shows that a systematic energy dependent error is to be expected in the intensities of the low energy region. This error is not included in the errors quoted in table 7. The fact that the conversion coefficient α_K of the 69.7 keV transition relative to the α_K(103.2 keV) agrees within 10–15 % with the values obtained in other experiments (see sect. 4), indicates that this systematic error is probably not much larger. Furthermore, when comparing neighbouring lines, only the error given in table 7 is the important one.

3.4. RESULTS OF THE LOW ENERGY PHOTO CONVERSION MEASUREMENTS

Most of the lines identified in the internal conversion experiments are also found in the external conversion measurements. In addition the spectrum shows the L conversion lines of the X-rays: Kα, Kβ'_1 and Kβ'_2. The line at 105 keV contains two or more gamma transitions and confirms that at least part of the lines in the group found at about 56 keV in the internal conversion spectra are K conversion lines. The mean gamma energy of this group of lines seems to be about 0.4 keV higher when computed from the external conversion spectrum indicating different intensity distributions of the groups. A new gamma ray is found at 151 keV. (The internal conversion K line of this gamma ray cannot be seen, since its energy corresponds to the N, O . . . lines of the 103.2 keV transition and the internal conversion L line was too weak to be observed.) When uranium converters were used, the L conversion lines of the 172.8 keV and the 151.5 keV transitions were found (table 8). The low energy photo conversion results are collected in table 7. The relative intensities obtained in the internal conversion measurement have been related to the intensities of the photo-conversion measurements by giving to the K 103.2 conversion coefficient the theoretical value corresponding to the experimental mixing ratio. In this way the total transition intensities have been calculated.

3.5. THE REGION FROM 220 TO 770 keV

Uranium oxide converters of 2.0, 3.3 and 6.0 mg/cm^2 were used generally. Lead converters were employed to discover possible K converted gamma rays masked by stronger L conversion lines. In this way it was possible to ob-

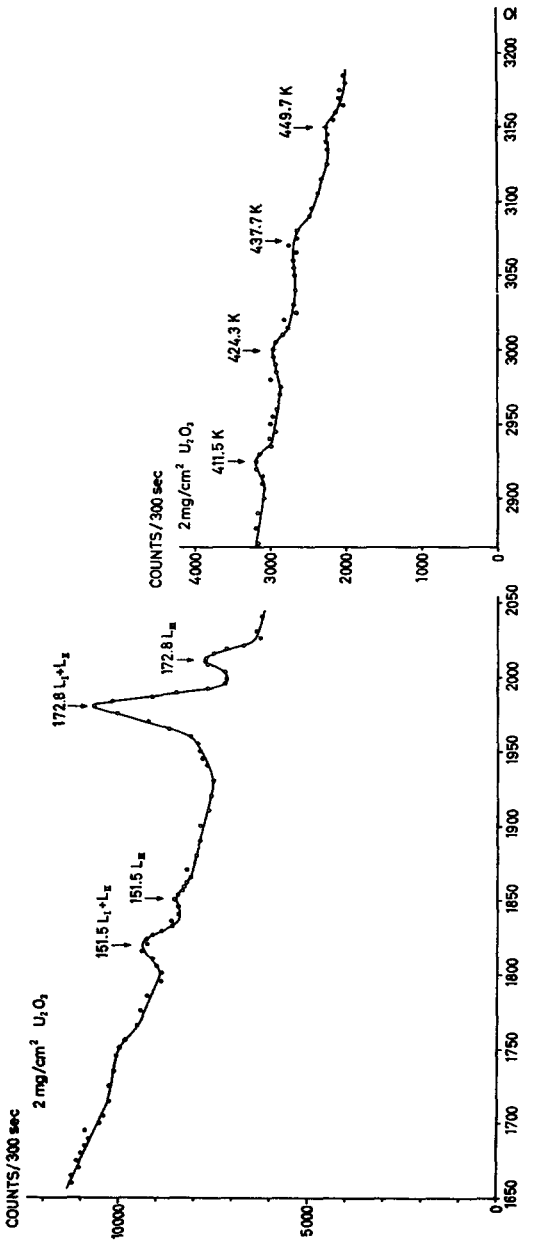

Fig. 4a. Photoconversion spectrum (4 %/60 resolution setting).

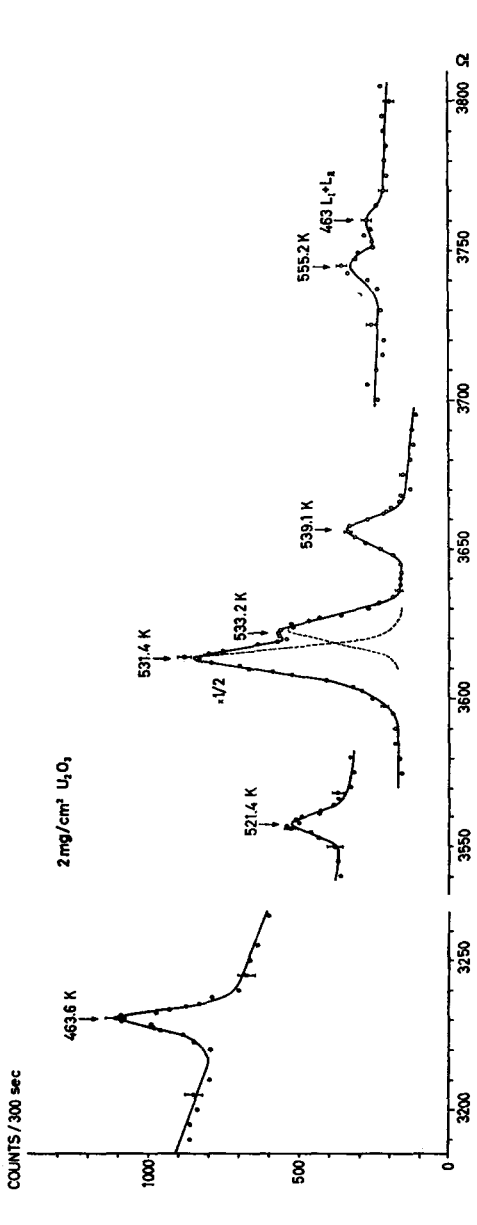

Fig. 4b. Photoconversion spectrum (2 %/60 resolution setting).

serve the 636 keV transition. Figs 4a, b, c and d show the spectrum measured with 2 mg/cm² converters. The weak lines were taken with a 4 mm wide converter and the spectrometer baffles adjusted for 0.4 % resolution. The stronger lines were recorded with a 2 mg/cm², 2 mm wide converter with the spectrometer adjusted for a resolution of 0.18 % (if no energy loss is present). With this setting a resolution of 0.27 % was obtained at 530 keV. At electron energies below 103 keV a very strong background due to scattering and conversion in the absorber is present. This prevents the detection of weak K con-

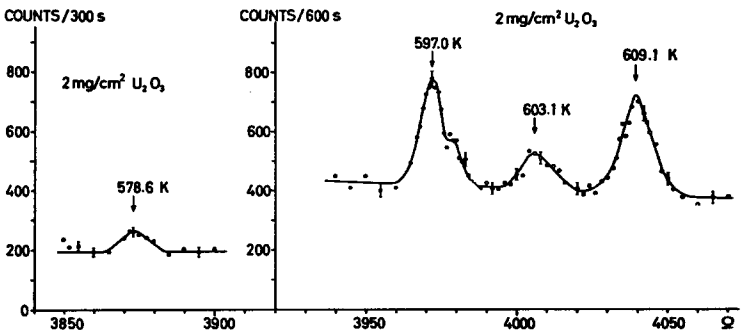

Fig. 4c. Photoconversion spectrum (2 ‰ resolution setting).

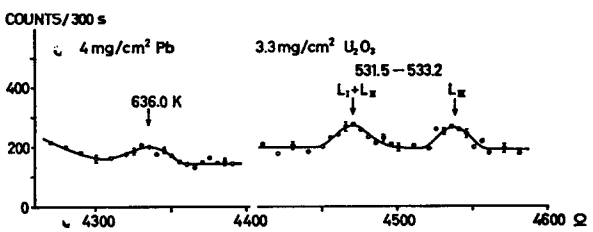

Fig. 4d. Photoconversion spectrum (4 ‰ resolution setting).

version lines of transitions below 219 keV when uranium converters are used. However, the L conversion lines belonging to the 151 and 172.8 keV transitions are seen clearly, but a large energy loss is present if a 2 mg/cm² converter is used. This is evident both from the shape of the lines and from the fact that the tops are shifted to lower energies by almost 0.5 keV.

The K 172.8 line (Sn converter) is observed in the low energy run and the L 172.8 line (U_2O_3 converter) is observed in the high energy run. The relative gamma intensities obtained in both runs were related using the value $\sigma_L/\sigma_K = 0.19 \pm 0.007$ given by Hultberg [22]) for uranium. We found

$$\frac{I_\gamma(531+533)}{I_\gamma(103.2)} = (33 \pm 7) \times 10^{-4}.$$

Since the ratio σ_L/σ_K is not accurately known, and the intensity determinations of the 172.8 keV lines contain rather large errors, another calculation was done using the data obtained from scintillation spectra taken with a multichannel analyser. Only the aluminium shielding necessary to stop the electrons was used in front of the 3.8 cm × 3.8 cm NaI(Tl) crystal and the absorption of the gamma rays was taken into account. It was found that the intensity ratio between the lines in the region 520 to 640 keV and the 103.2 keV gamma ray is $(56\pm7)\times10^{-4}$. Values reported by previous investigators are given in table 10. Using the relative high-energy intensities from the external conversion measurements we obtain

$$\frac{I_\gamma(531+533)}{I_\gamma(103.2)} = (40\pm10)\times10^{-4}.$$

The agreement between the determinations with the two methods was considered satisfactory. A value of 35×10^{-4} was used to match the low and high energy intensities given in tables 7 and 8.

3.6. RESULTS OF THE HIGH ENERGY PHOTO-ELECTRON MEASUREMENTS

The results are summarized in table 8. A number of lines not reported up till now have been detected. The 530 keV and the 600 keV gamma rays reported in earlier works are seen to be composed of several lines. The region between 636 keV and 770 keV was carefully studied with a 6 mg/cm² uranium converter, but no line was found. Gamma rays eventually existing in the region 636 to 770 keV and not reported in table 8 must have an intensity smaller than 1×10^{-4} of the intensity of the 103.2 keV gamma transition.

The 600 keV group is composed of three gamma rays of energy 596.9, 603.1 and 609.1 keV, but the first seems to be double with an additional, weaker gamma ray at 598.2 keV.

Numerical sum relations of the type $E_1+E_2 = E_3+E_4 = E_5$ may give some information about possible high energy levels in Eu^{153}. The energies obtained from the external conversion experiments for a group of four gamma rays suggest within the limit of errors the existence of a level at 636.4 keV which decays to the 172.8, 103.2, 97.5 keV levels and to the ground state through the following transitions: 463.6, 533.2, 539.1, 636.0 keV. Two levels at 706.4 and 694.3 keV respectively are also suggested decaying by two pairs of cascading gamma rays 609.1+97.5 and 603.1+103.2 keV from the first level and 596.9+97.5 and 521.3+172.8 keV from the second. No relationship of this type could be found for the strongest high energy transition (531.4 keV). The seven other lines found above 400 keV have an intensity smaller than 2×10^{-4} of the 103.2 keV line. None of them can be placed in the present decay scheme from sum relations only.

TABLE 9

K conversion coefficients

Authors	Method	Transitions (keV)							Mother isotope
		69.7	75.3	83.4	89.4	97.5	103.2	172.8	
Siegbahn [28])	coinc.						0.65		Sm^{153}
Graham and Walker [29])	coinc.	5.7±1.0							Sm^{153}
Lee and Katz [11])	coinc.						0.62±0.15		Sm^{153}
McGowan [30])	coinc.	3.8±0.2					1.14±0.20		Sm^{153}
Marty [10])	coinc.						1.2 ±0.1		Sm^{153}
Dubey *et al.* [6])	coinc.	4.4±0.4					1.19±0.15		Sm^{153}
Joshi *et al.* [31])		3.5±1.4					0.69±0.08		Sm^{153}
Marty and Vergnes [32])	coinc.					0.3±0.1			Gd^{153}
Bernstein and Lewis [44])				3.6					Coul.exc.
Sund and Wiedenbeck [33])	coinc.	4.4±0.3				$0.36^{+0.03}_{-0.07}$	1.16±0.08		Sm^{153}
Present measurement [a,b])	int. ext. conv.	4.0±0.3	0.41±0.07	3.6±0.6	3.8±0.5	0.35±0.04	1.43	0.27±0.03	Sm^{153}
Present measurement [a,b])	coinc.	4.5±0.4					1.50±0.15		Sm^{153}
Theoretical value		4.41 [b])	E1 0.51	2.35 [b])	M1 2.17 E2 1.5	E1 0.256	1.43 [b])	M1 0.34 E2 0.24	

[a]) Our relative values are normalized to $\alpha_K(103.2\ \text{keV}) = 1.43$ determined from Sliv's tables.

[b]) The mixing ratio determined from L subshell ratios was assumed.

4. Conversion Coefficients

Relative K conversion coefficients are calculated from the internal and external conversion intensities (table 9). The values are normalized by giving to $\alpha_K(103.2)$ its theoretical value for the multipole mixture obtained from its L subshell ratios given in table 5. Thus the obtained experimental conversion coefficients can be directly compared to the theoretical conversion coefficients. The theoretical values have been obtained using the mixing ratios determined from L subshell ratios whenever these ratios could be measured.

The fact that the experimental K conversion coefficients of the 89, 83, 75 keV differ from the theoretical values [18]) twice the given statistical error cannot be considered too significant. For the 69.7 keV transition we get 10 % smaller value, and this may be partially accounted for some systematic error in the external conversion method, when it is applied to low energies.

We have also performed a determination of the conversion coefficients $\alpha_K(69)$ and $\alpha_K(103)$ using gamma-gamma coincidence measurements. When we select the 69.7 keV gamma ray in one channel, we obtain in the coincidence spectrum the 103.2 keV gamma and the KX-rays (with an intensity $\alpha_K\omega_f, I_\gamma(103)$). Other contributions to the X-rays are negligible. Absorption, escape peak, and efficiency of the coincidence circuit were taken into account in the computation of the intensities. The fluorescence yield ω_f, was taken equal to 0.91 (ref. [41])). Our result was

$$\alpha_K(103.2) = 1.50 \pm 0.15.$$

In a similar way we obtained

$$\alpha_K(69.7) = 4.5 \pm 0.4.$$

Values of the 103.2 keV K conversion coefficient reported by earlier investigators are given in table 9. They seem to group around two values: 0.65 and 1.1. The first group of values is in complete contradiction with the present measurements. The second group have α_K values somewhat lower than ours but indicate a rather pure E2 transition. The present value 1.5 fits with the assumption of a pure M1 transition, and agrees with the δ^2 value obtained from K/L and $(L_I+L_{II})/L_{III}$ ratios.

TABLE 10

Relative gamma intensities ($I_{103.2} = 100$)

Authors	Method	69.7	172.8	463	530	600
Beckman [7])	crystal sp.	9				
Mc Cutchen [24])	proport. counter	20			0.5	0.1
Dubbey *et al.* [6])	scint.	25	0.073		0.15	0.036
Anderson [25])	scint.	10				
Kløve *et al.* [26])	scint.	31	0.14		0.31	0.08
Marty [10])	scint.				0.7–1.0	
Sund and Wiedenbeck[23])	scint.	13	0.18	0.05	0.48	0.1
Present work		19	0.33	0.055	0.44	0.12

5. Electron-Gamma and Beta-Gamma Coincidence Measurements

5.1. INSTRUMENTAL CONDITIONS

The aim of our coincidence measurements was to find some high energy levels of Eu^{153} and specially to confirm the existence of the 636.4, 694.3 and 706.4 keV levels suggested in subsect. 3.6. A quantitative analysis of the coincidence data was performed in order to be able to give to the stronger transitions a unique position in the decay scheme.

The measurements were performed with a magnetic lens spectrometer [37]) and a gamma scintillation spectrometer with a 6.4 cm diam. by 5.1 cm height NaI(Tl) crystal. The magnetic spectrometer was set at a resolution of 4.8 %. The electron lines to be selected, K 97.5, K 103.2 and L 69.7, were then clearly resolved.

The gamma spectrum coincident with the selected electron line was collected in a RIDL 400-channel pulse-height analyser. A resolving time of $2\tau = 5 \times 10^{-8}$ sec was chosen in the coincidence circuit in order to obtain a constant coincidence efficiency over a wide gamma energy range (150 to 700 keV). Single spectra were taken after each coincidence run, without observing any calibration shift. When the high energy gamma spectrum was studied, an absorber of 0.5 mm lead and 0.5 mm tin was used to reduce the intensity of the strong low energy lines. The source-to-crystal distance was then 29 mm. The low energy single gamma ray spectra were taken at a distance of 91 mm and without any absorber. The source was located in an aluminium cup of 0.7 mm wall thickness, open to the spectrometer vacuum tank. The cup, and the NaI crystal can and reflector material were sufficient to stop all the electrons. The source was obtained irradiating isotopically enriched Sm_2O_3 in a flux of 2×10^{12} neutrons per $cm^2 \cdot$ sec. After irradiation it was evaporated onto a 0.7 mg/cm^2 aluminium foil.

5.2. QUANTITATIVE ANALYSIS OF THE COINCIDENCE SPECTRA

In an electron-gamma coincidence experiment we focus a line u in the electron channel and obtain the gamma spectrum coincident with u. We call $N_c(u; v)$ the number of counts obtained by integrating the coincidences registered in a photopeak. Random coincidences and Compton backgrounds from other lines coincident with u are previously subtracted. Then

$$N_c(u; v) = \varepsilon_c N_u \eta_v \varepsilon_v a_v \delta(u; v) = \varepsilon_c N_v \omega \alpha(u) \delta(v; u),$$

where N_u is the number of counts belonging to the line u accepted by the electron channel (N_u is generally the peak-counts of a conversion line; backgrounds are subtracted), N_v the number of counts integrated over the photopeak (backgrounds subtracted) that is accepted by the gamma-channel, ε_c the efficiency of the coincidence circuit, η_v the crystal efficiency, ε_v the photo-

peak-to-total ratio (corrections due to escape peaks of the low energy gamma rays must be included), a_v the gamma ray absorption factor $= e^{-\mu x}$, ω the transmission of the beta spectrometer, $\alpha(u)$ the conversion coefficient corresponding to u, $\delta(u; v)$ the fraction of transition u coincident with gamma transition v, $\alpha(u)\delta(v; u) = \alpha(u)[I(u)/I(v)]\delta(u; v)$ the fraction of transition v coincident with transition u, selected in the beta spectrometer, I the gamma intensity.

The quantities δ can be calculated from transition intensities, conversion coefficients and an assumed decay scheme. The experimental values of δ obtained from the coincidence measurements then test the validity of the decay scheme assumed. The quantities δ may be obtained either from the first or from the second equation. We preferred the second since ω was known with higher accuracy than $\eta_v\varepsilon_v a_v$, and two different source-to-crystal distances were used.

In general more than one line is accepted in the electron channel; then we have $N_U = \sum_u N_u$, where N_u are the counts corresponding to each of the lines u that contribute to the counts N_U. We may also have, both in the single gamma spectrum and in the coincidence spectrum, a group V of unresolved photopeaks which cannot be decomposed into its components ($N_V = \sum_v N_v$). In such a case we have for the whole group V coincident with U:

$$N_c(U; V) = \sum_{u,\,v} N_c(u; v) = \varepsilon_c \sum_{u,\,v} N_u \eta_v \varepsilon_v a_v \delta(u; v) = \varepsilon_c \sum_{u,\,v} N_v \omega \alpha(u) \delta(v; u).$$

These equations cannot be solved to obtain the quantities δ, since we know N_U, N_V and $N_c(U; V)$, but not N_u, N_v and $N_c(u; v)$. However, the values N_v may be computed if the gamma intensities of the different lines composing V are known from another experiment (in our case, the external conversion measurements). These intensities can be transformed into photopeak intensities taking into account crystal efficiency, peak-to-total ratio, escape peak, absorption, etc.; the number of counts N_v corresponding to each line in the group with N_V counts is then easily obtained. When $\varepsilon_v\eta_v a_v$ can be considered constant for the lines of the group, we may write directly $N_v = N_V I_v / \sum_v I_v$ and then

$$N_c(U; V) = \varepsilon_c N_V \omega \sum_u \alpha(u) \frac{\sum_v I_v \delta(v; u)}{\sum_v I_v}.$$

In many cases it is possible to separate the contribution to N_c due to different radiations in the electron-channel and then $N_c(u; V)$ is determined. In our case the contribution due to the continuous beta spectrum was obtained by measuring the spectrum coincident with the electrons of energy above the L 69.7 line. The contribution from L 69.7 and K 97.5 in N_c(K 103.2; 530) could be neglected because N_c(L 69.7; 530) and N_c(K 97.5;

530) are much smaller; when measuring N_c(L 69.7; 530) or N_c(K 97.5; 530) the contribution of K 103.2 to N_c could be computed from the preceding measurement. Another experiment was done to estimate a possible contribution due to the K 105 transition. The magnetic spectrometer was first set to select an energy around the K 105 line and then a second coincidence spectrum was taken with the spectrometer set at the low energy slope of the K 103.2 line, so as to have the same single counting rate in both cases. No difference was observed in the shape of the coincidence spectrum, showing that the 105 keV line has a small contribution, if any, to the coincidence spectrum. The transmission ω in our beta spectrometer is known with an accuracy of 10 to 15 % from many earlier experiments and is rather insensitive to small changes in the size of the source. The transmission is energy dependent because of the variation of the line shape with energy. We have, however, assumed ω to be a constant considering that all the measured conversion lines are rather close: Furthermore no big change is to be expected in ω for the L and the K conversion lines with the resolution used in the experiment.

The half-life of all the levels involved in the experiment was considered to be short compared to the 2τ-value of the coincidence circuit. This is actually the case for the 97.5, 103.2 and 172.8 keV levels [29, 30, 42, 43]).

5.3. RESULTS OF THE ELECTRON-GAMMA COINCIDENCE MEASUREMENTS

The electron-gamma coincidence spectra are shown in fig. 5. The coincidence counting rate corresponding to photopeaks in the 460, 530 and 600 keV regions are reported in table 11. This counting rate has been corrected for contributions from other coincidences than those produced by the rays quoted in column one and two of table 11. The experimental values

$$\frac{N_c(u;V)}{N_V \varepsilon_c \omega} = \alpha(u) \frac{\sum_v I_v \delta(v;u)}{\sum_v I_v}$$

are compared to the values calculated assuming the decay scheme in fig. 7. The values obtained by placing some transitions in another way into the decay scheme are given in the last column.

There is a reasonable agreement between the values in column 4 and 5, that is between the experiments and the proposed decay scheme. Comments on some details are however needed. The low value obtained for the experimental δ (103.2; 69.7) might be partially due to a small change coincidence efficiency for the low energy gamma rays. The analysis shows that the 531 and 533 keV rays go to the 103.2 keV level but not the ground state, nor to the 97.5 keV or the 172.8 keV level. A comparison of the line shape of the coincidence peak (K 103.2; 530) with the annihilation peak of Na^{22} shows a small contribution in the 600 keV region. The intensity indicates that one

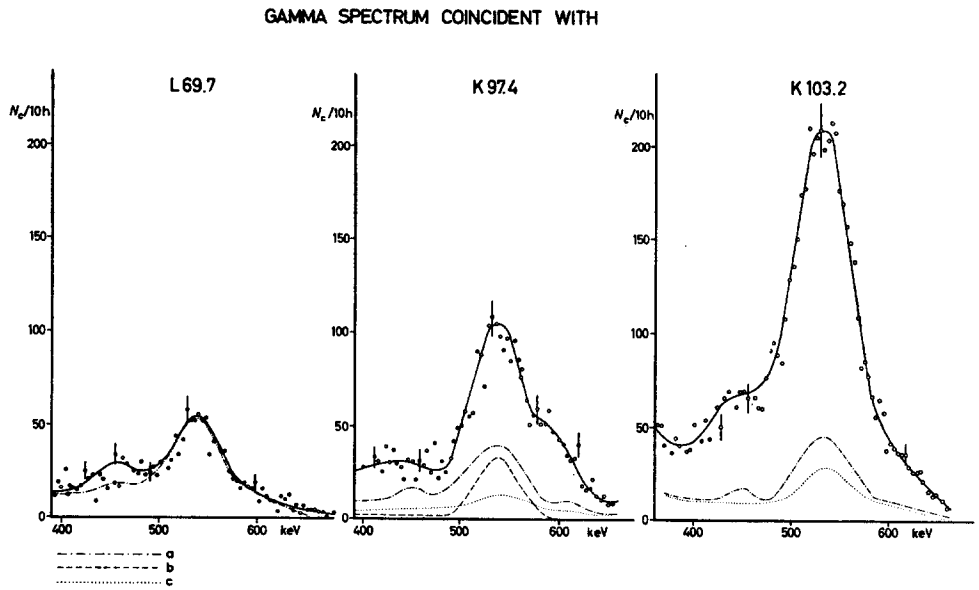

Fig. 5. Electron-gamma coincidence spectra. The curves a, b and c represent: a — Contribution of the continuous beta spectrum. b — Random coincidences. c — Contribution of the K 103.2 line to the gamma spectrum coincident with K 97.5.

TABLE 11

Coincidence results

Electron transition selected in the beta spectrometer (keV) (u)	Coincident gamma energy (keV) (v)	Coincidence rate (N_c per 10 h)	$\alpha(u)\frac{\Sigma I_v\,\delta(v;u)}{\Sigma I_v}$		
			Exp.	Calculated	
			$\frac{N_c}{\varepsilon_c\,\omega\,N_v}$	According to proposed decay scheme	The same decay scheme except for the quoted transition to another state
L 69.7	463	135±50	0.09 ±0.04	0.12	
	530	<70	<0.009	0.0065	0.06 (531 to 172)
	600	<30	<0.015	0	0.05 (597+609 to 172)
K 97.5	463	<100	<0.07	0	0.19 (463 to 97)
	530 + 600	760±200	0.060±0.015	0.045	0.123 (531 to 97)
K 103.2	463	600±200	0.40 ±0.15	0.52	
	530	4120±300	0.390±0.085	0.394	0.135 (531 to gr. st.)
	600	200±100	0.094±0.05	0.064	0.17 (597+609 to 103)
L 69.7	103.2	6440±600[a])	0.031±0.005	0.056	
K 103.2	69.7	2910±300[a])	0.31 ±0.05	0.52	

[a]) These two values give N_c per hour, instead of per 10 h.

of the weaker lines of the 600 keV group is directly or indirectly feeding the 103 keV level. Since no coincidences (L 69.7; 600) are seen, we have tentatively placed the 603.1 keV line on top of the 103.2 keV level. The 97.5 keV level is in coincidence with the 530 and 600 keV regions; the intensity of the first one seems to be somewhat lower than the 600 keV region. Intensity considerations indicate that the two strongest lines of the 600 keV group (569.9 and 609.1 keV) probably go to the 97.5 keV level. The position given to the 463 keV line in the decay scheme is supported by the (L 69.7; γ) coincidences. Because of the relatively strong contribution of the continuous beta spectrum a possible 521.3 keV-69.7 keV cascade can not be excluded. A coincidence experiment with K 83 showed that none of the strong high energy gamma rays are coincident with this transition. The weakest lines in the 500 group (578.6 keV, 555.2 keV) could not be placed by the coincidence measurements and that is also the case for four weak gamma rays in the 400 keV group, each with an intensity of the order of 0.01 % ($I_\gamma(103.2) = 100$ %).

5.4. BETA-GAMMA COINCIDENCES

Beta-gamma measurements were performed to obtain an additional proof that the 530 keV transitions does not go directly to the ground state. With a resolution of 12 % in the beta channel, the coincidences (130 keV; γ) and (200 keV; γ) were measured. A 530 keV line was clearly seen in the first case, but not in the second, where it must be at least seven times smaller. Together with the measured Q value of around 810 keV, this means that the 531 and 533 keV transitions both decay from levels above 600 keV.

5.5. GAMMA-GAMMA COINCIDENCE EXPERIMENTS

Our gamma-gamma coincidence experiments confirm some of the results obtained with electron-gamma coincidence. Five coincidence spectra were taken: (580-620 keV; γ), (510-550 keV; γ), (420-470 keV; γ), (96-109 keV; γ) and (65-73 keV; γ) with an 80-channel analyzer. They are shown in fig. 6a and b. The first three spectra show that the 600 keV and the 530 keV regions give coincidences with the 97.5+103.2 keV line, but not with the 69.7 keV transition; the 460 keV region is in coincidence with the 103.2 and the 69.7 keV transitions. In the first two cases the ratio of the 97.5 keV to the 103.2 keV intensity was computed from the X-ray to 97.5+103.2 keV intensity ratio. The 600 keV is found to be mainly in coincidence with the 97.5 keV line, the contribution to the 103 keV line is at least to a large extent due to the tail of the 530 keV lines. In the (530; γ) spectrum (65$\pm$10)% of the composite peak corresponds to the 103.2 keV line. If we assume that in channel I we select only the 531.4, 533.2 and the 539.1 keV lines, then our decay scheme gives a value of 70 %. The (463; γ) spectrum shows a still stronger X-ray peak compared to the 103.2 keV line because of the presence of the coincident 69.7 keV line.

The (96-109 keV; γ) coincidence spectrum has a similar shape to the single spectrum, except for the intensity of the 600 keV group which is somewhat higher. From subsect. 5.2 it follows that $N_c/N_V \propto 1/(1+\alpha_T)$. This factor is larger by a factor of two for the gamma rays in coincidence with the 97.5 keV

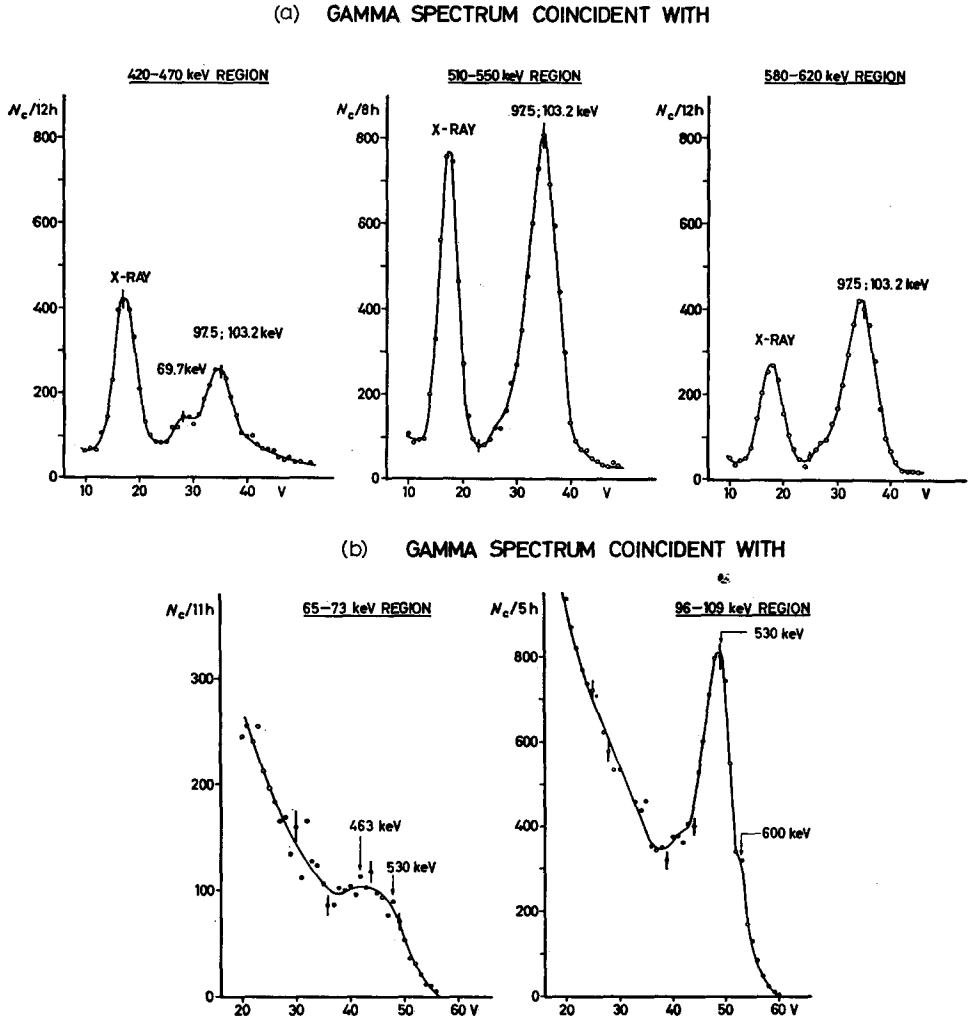

Fig. 6. Gamma-gamma coincidence spectra. Random coincidences are subtracted.

transition compared to those in coincidence with the 103.2 keV ray. As concluded in last paragraph all the strong lines in the 600 keV region are in coincidence with the 97.5 keV line. The 600 keV line should then appear much stronger in the coincidence spectrum than in the single spectrum compared to the 530 keV lines, just as observed in fig. 6b. The (65-73 keV; γ) spectrum

shows clearly the 460 keV line and a contribution of about the same intensity in the 530 keV region. This is due to the escape peaks of the 97.5 keV and 103.2 keV lines which both are in coincidence with the gamma rays of the 530 keV region.

After we had finished our gamma-gamma measurements, a paper by Sund and Wiedenbeck [33]) was published, which shows that a large amount of information may be obtained with only gamma-gamma coincidence techniques. The authors report several transitions not published earlier. The rays of 154, 422 and 458 keV may be considered identical with our 151.5, 424.3 and 463.6 keV gamma transitions; a ray at 352 keV is not seen by us [this means $I_\gamma(352) \leqq 1\times10^{-4}\times I_\gamma(103.2)$] and their rays of 67 and 525 keV are obtained by a qualitative analysis of the coincidence spectra which does not agree with our conclusions. The accurate energy values, the possibility of resolving neighbouring lines in photoconversion experiments and the quantitative analysis of the coincidence spectra has led us to a different decay scheme for the high energy part. Some discrepancies with Sund and Wiedenbeck's work may be explained by a more quantitative analysis of their results. The authors assume the existence of a 525 keV transition to explain the decreased intensity ratio of the 535 keV to the 610 keV transition in the coincidence spectrum with the 103-97 keV lines, compared to the ratio in the single spectrum. The intensity change follows, however, from the fact that

$$\frac{\delta(530;\ 103.2)}{\delta(600;\ 97.5)} = \frac{(1+\alpha_T\ 97.5)}{(1+\alpha_T\ 103.2)} \approx \tfrac{1}{2}.$$

The 67 keV line found by Sund and Wiedenbeck in coincidence with the 445-475 keV region is according to our interpretation identical with the 69.7 keV line. We did not see any 67 keV line either in our internal or external conversion experiments. The 103 keV line seen in the 445-475 keV coincidence spectrum is, according to these authors, due to the Compton background of the 531 keV line, which they estimate to about 40 % of the total counts in the 445-475 keV region. Now, if we assume that the 463 keV ray is followed by the 69.7 keV transition, this Compton background contributes to the coincidence counting rate in the ratio $N_c(103.2)/N_c(69.7) \approx 1.5$ [since $\delta(530;\ 103.2)/\delta(463;\ 69.7) \approx 2$]. However, their coincidence spectrum shows a 103 keV line which is several times stronger than the 69 keV line, which clearly indicates that the 463 keV region is in coincidence with the 103.2 keV gamma ray. It is much more difficult to interpret the $(172.8;\ \gamma)$ coincidence spectrum that they obtained when the 166-191 keV region was selected, since no quantitative analysis is made. This spectrum shows lines at 154, 352, 422 keV (supposed to be in coincidence with the 172.8 keV line), but no line at 463 keV which is in complete disagreement with our decay scheme. However, this experiment is very difficult to perform. From the branching ratios of the

69.7 to 172.8 keV transitions we deduce that $\delta(\gamma; 172.8) = I_\gamma(172.8)/I_\gamma(69.7) \times (1+\alpha_T\ 69.7) \approx 3\times 10^{-3}$. Very small coincidence counting rates should be obtained; particularly for lines as weak as the 422 keV (if it is identical with our 424). The counting rate should be of the order of 10^{-4} smaller than $N_c(103; 530)$ for the same geometry, source strength and sampling time. In their spectra Sund and Wiedenbeck have $N_c(103; 530)/N_c(172; 422) \approx 5$, but no information is given for the factors just mentioned. The main difficulty comes from spurious contributions in the 166-191 keV channel (Compton background, bremsstrahlung, 191 keV line and other weak lines (171 keV?)). If they belong to a cascade with a δ value of the order of unity they may give rise to much stronger coincidence peaks, even if their single counting rates in the 166-191 keV channel is very small compared to the 172.8 keV line. Hence, it becomes very difficult to draw any definite conclusions from their coincidence spectrum.

6. Discussion

The proposed decay scheme of Sm^{153} to Eu^{153} is shown in fig. 7. The transition intensities (in transitions per hundred decays) and log ft values have been calculated assuming the intensity of the beta component to the ground state to be 20 %. (See table 1 and ref. [1])). The ground state of Sm^{153} has a directly measured [3]) spin of $I = \frac{3}{2}$. It is identified with a single particle state with the Nilsson asymptotic quantum numbers $\frac{3}{2}-[521]$ and has a deformation parameter $\delta \approx 0.25$. The ground state spin of Eu^{153} is also measured directly [4, 5]) giving $I = \frac{5}{2}$. This state is best characterized with the quantum numbers $\frac{5}{2}+[413]$. Its deformation parameter is determined to $\delta = 0.32\pm 0.05$ from Coulomb excitation work [45]), while ${}_{63}Eu^{151}_{88}$ has a $\delta \approx 0.16$, stressing the sharp increase in nuclear eccentricity when going from neutron number $N = 88$ to 90. There are two minima in the curve of energy as function of deformation $E = E(\delta)$, and the shift from one minimum to the other occurs when the neutron orbital $\frac{1}{2}+[660]$ is filled. This shift of minimum in going from Eu^{151} to Eu^{153} leads also to the observed increase of Q-value with about a factor of two. For Eu^{153} ($N = 90$) we may also encounter excited configurations with smaller deformation showing up in decreased transition probabilities. The asymptotic quantum numbers n_z and Λ are strictly valid only in the limit of large deformation. For a δ-value of about 0.3 the calculated states usually correspond to the asymptotic states with an accurary of about 90 %.

The Alaga gamma intensity rules are valid for enhanced transitions but not for hindered transitions, reflecting the fact that the hindered transitions are extremely sensitive to very small admixtures in the nuclear wave function. We thus expect deviations from the theoretical transition rules both because of changes in nuclear deformation and because of configuration mixing.

6.1. LEVELS BELOW 200 keV

The assignments of the low energy levels in fig. 7 are the same as those proposed by Mottelson and Nilsson in fig. 1.

The ground state configuration $\frac{5}{2}+[413]$ has a $\frac{7}{2}+$ rotational member at 83.37 keV and a probable $\frac{9}{2}+$ member at 191.4 keV (cf. discussion on the 108.0 keV transition in sect. 2). The simple rotational formula without cor-

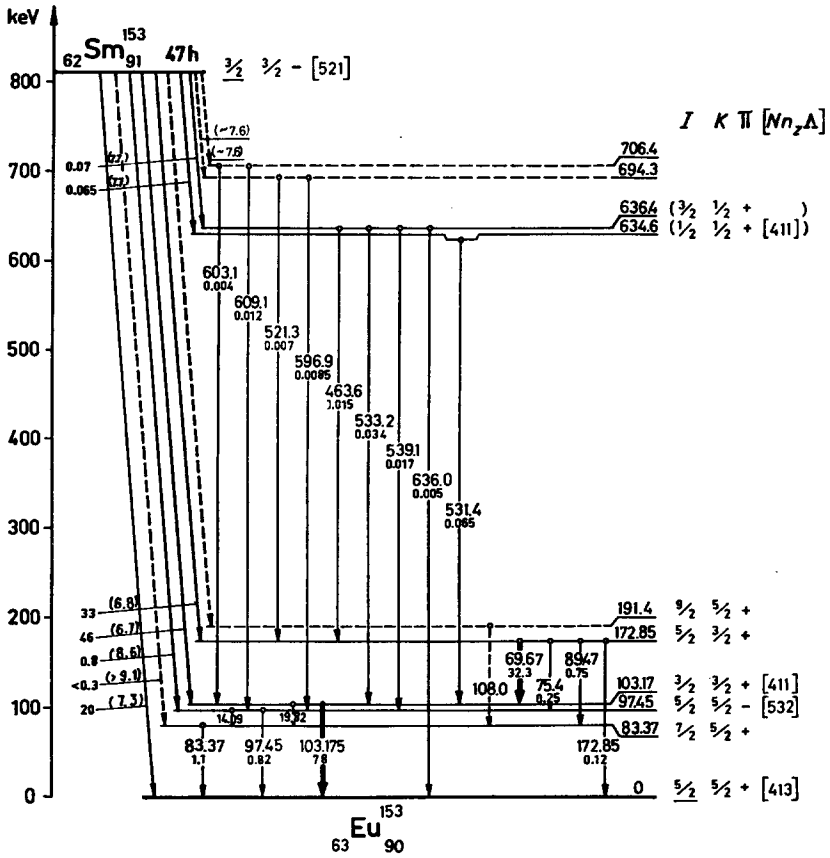

Fig. 7. Proposed decay scheme. Total transition intensities are given in transitions per hundred decays. The log *ft* values are given in parenthesis.

rection for interactions gives an energy of 190.5 keV for the $\frac{9}{2}$ member. The energy deviation indicates band mixing. The 97.45 keV level de-excites with an E1 transition to the ground state and with an 14.09 keV (E1) transition to the 83.37 keV $\frac{7}{2}+$ level. Its spin-parity is thus $\frac{5}{2}-$ or $\frac{7}{2}-$. The only neighbouring negative parity single particle state in the Nilsson diagram (fig. 3 of ref. [2])) is the $\frac{5}{2}-[532]$ state (approaching the ground state with smaller eccentricity if it is a hole state). Mottelson and Nilsson explain the weak beta feeding to

this level as caused by a considerable change in the nuclear shape. The de-exciting transitions should be strongly hindered by the asymptotic quantum numbers and table 9 shows an increased experimental conversion coefficient α_K (97.5) compared to a pure E1 transition value. An accurate measurement of the L subshell ratios and a half-life determination of the 97.5 keV level would be of considerable interest. The 103.17 keV level is best characterized by the single particle level $\frac{3}{2}+$ [411] with its first rotational level at 172.85 keV ($I = \frac{5}{2}$). The strong transitions of 69.67 and 103.17 keV are both of almost pure M1 character (98.9 % and 98.1 % M1 respectively). Graham *et al.*[12]) have reported that the branching from the 172.85 keV level to the ground state rotational band does not agree with the theoretically expected ratio for allowed transitions. Such effects may be expected as mentioned earlier.

The half-life of the 103.2 keV level has been measured by many authors[29, 30, 42, 43]). The value $T_{\frac{1}{2}} = 3.3$ nsec by P. Reyes-Suter and T. Suter together with the measured multipolarity (98.9 % M1) gives a hindrance factor of

$$H_{M1} = \frac{\lambda(\text{theory})}{\lambda(\text{exp.})} = 420$$

for this transition, λ(theory) being Moszkowski's single-particle transition probability estimate.

The half-life of the 172.8 keV level is measured by Graham and Walker [29]), who obtained 0.14 nsec. With the multipolarity given in table 5 for the 69.7 keV transition we obtain a hindrance factor of

$$H_{M1} \approx 12.$$

6.2. LEVELS ABOVE 200 keV

The positions of the 634.6 and 636.4 keV levels are supported both from coincidence data and from numerical sum relations. The log *ft* values of the beta branches feeding these levels suggests spins $\frac{1}{2}$, $\frac{3}{2}$ or $\frac{5}{2}$. The 634.6 keV level decays strongly to the 103.17 keV level of spin $\frac{3}{2}$. A weak transition to the ground state [$I_\gamma(634.6) < 10^{-1} \times I_\gamma(531.4)$] is probable, but it would not be resolved in our spectrum from the 636.4 keV transition. The other low energy levels (with $I = \frac{5}{2}, \frac{7}{2}, \frac{9}{2}$) are not observed to be fed from the 634.6 keV level. Hence its spin is probably $\frac{1}{2}$. The 636.4 keV level decays to all the low energy levels except for the $\frac{7}{2}$ and $\frac{9}{2}$ levels. A probable spin assignment would thus be $\frac{3}{2}$ or $\frac{5}{2}$. The 634.6 and 636.4 keV levels may then be identified with the single particle level $\frac{1}{2}+$ [411] and its first rotational member $I = \frac{3}{2}$ based on it. The intensities of the different transitions involved are in reasonable agreement with this assignment except for the relatively strong transition to the 97.45 keV level ($I = \frac{5}{2}-$). The small separation of only 1.8 keV between

the 634.6 and 636.4 keV levels causes a large negative decoupling parameter

$$a_{\text{exp}} = -0.954 \pm 0.011,$$

in good agreement with the theoretical value of

$$a_{\text{theory}} = -0.9$$

for $\delta \approx 0.26$. The decoupling parameter is of special interest since it depends on the details of the intrinsic motion and can be explicitly calculated in terms of the last odd nucleon.

The third member ($I = \frac{5}{2}$) of this band will have an excitation energy of about 760 keV and would thus be very weakly fed. This position is calculated assuming a mean of the moment of inertia of the ground state band $3\hbar^2/J = 71.48 \pm 0.02$ and the band starting at 103 keV with $3\hbar^2/J = 83.61 \pm 0.01$ The small splitting of the 634.6 and 636.4 keV levels makes the possibility of assigning this band a gamma vibrational character improbable.

The two levels at 694.3 and 706.9 keV decay mainly to the 97.5 keV level. According to the Nilsson diagram for single particle levels of odd-proton nuclei the remaining hole and particle excitation levels below about 800 keV are $\frac{7}{2}-[523]$, $\frac{3}{2}+[404]$ and $\frac{3}{2}-[541]$. The beta transitions to the first two of these levels are second and third forbidden and cannot be excited here. The $\frac{3}{2}-[541]$ state may be a possible assignment of one of the two levels around 700 keV and the other level could tentatively be interpreted as a gamma vibrational level based on the $\frac{5}{2}-[532]$ state. Several other levels must however also exist to account for the remaining gamma rays observed and not placed in the present decay scheme. This may be considered as an indication of several vibrational levels excited in this nucleus.

The authors wish to express their gratitude to Professor Kai Siegbahn for the excellent facilities put to their disposal. We are indebted to W. C. Parker for many skilful source and converter preparations. Two of us (T. S. and P. S) like to acknowledge scholarships from the Argentine Consejo Nacional de Investigaciones Científicas y Técnicas. The work has been financially supported by the U.S. Air Research and Development Command.

References

1) Nuclear Data Sheets, National Academy of Sciences, National Research Council, Washington D.C.
2) B. R. Mottelson and S. G. Nilsson, Mat. Fys. Medd. Dans. Vid. Selsk. **1**, No. 8 (1959) 105
3) A. Cabezas, E. Lipworth, R. Marrus and J. Winoeur, Phys. Rev. **118** (1960) 233
4) J. E. Mack, Rev. Mod. Phys. **22** (1956) 64
5) B. Bleaney and W. Low, Proc. Phys. Soc. **68A** (1955) 55
6) V. S. Dubey, C. E. Mandeville and M. A. Rothman, Phys. Rev. **103** (1956) 1430
7) O. Beckman, Nuclear Instruments **3** (1958) 27

8) P. Bergvall, Arkiv f. Fysik **17** (1960) 125
9) I. J. Walters, J. H. Webber, N. C. Rasmussen and H. Mark, Nuclear Physics **15** (1960) 653
10) N. Marty, J. Phys. Rad. **16** (1955) 458
11) M. Lee and R. Katz, Phys. Rev. **93** (1954) 155
12) R. L. Graham, G. T. Ewan and J. S. Geiger, Bull. of Am. Phys. Soc. **5** (1960) 21 and private communication
13) A. Moussa and E. Monnand, J. Phys. Rad. **21** (1960) 463
14) A. Hedgran, K. Siegbahn and N. Svartholm, Proc. Phys. Soc. **63** (1950) 960
15) G. Bäckström, Nuclear Instruments **1** (1957) 253
16) K. Siegbahn and K. Edvarson, Nuclear Physics **1** (1956) 137
17) P. Bergvall and S. Hagström, Arkiv f. Fysik **17** (1960) 61
18) L. A. Sliv and I. M. Band, Coefficients of internal conversion of gamma radiation (Moscow-Leningrad, 1958)
19) E. M. Bernstein and R. Graetzer, Phys. Rev. **119** (1960) 1321
20) C. M. Class and U. Meyer-Berkhout, Nuclear Physics **3** (1957) 656
21) K. M. Glover and P. Borrell, J. Nuclear Energy **1** (1955) 214
22) S. Hultberg, Arkiv f. Fysik **15** (1959) 307
23) G. White Grodstein, Nat. Bureau of Standards, Circular 583 (1957)
24) E. P. Grigor'ev and A. V. Z. Zolotavin, JETP (Sov. Phys.) **36** (1959) 272
25) R. H. Pratt, Phys. Rev. **119** (1960) 1619
26) G. D. Latyshev, Revs. Mod. Phys. **19** (1947) 132
27) F. Sauter, Ann. Phys. **11** (1931) 454
28) K. Siegbahn, Arkiv f. Fysik **4** (1952) 223
29) R. L. Graham and J. Walker, Phys. Rev. **94** (1954) 794 A
30) F. K. McGowan, Phys. Rev. **93** (1954) 163
31) M. C. Joshi, B. N. Subba Rao and B. V. Thosar, Proc. Indian Acad. Sci. **45 A** (1957) 3
32) N. Marty and M. Vergnes, Compt. Rend. **242** (1956) 1438
33) R. E. Sund and M. L. Wiedenbeck, Phys. Rev. **120** (1960) 1792
34) C. W. McCutchen, Nuclear Physics **5** (1958) 187
35) B. Andersson, Proc. Phys. Soc. **69 A** (1956) 415
36) A. Kløve and A. Storruste, Arkiv Math. Naturvidenskab. B. Liv. **6** (1958)
37) T. R. Gerholm and B. G. Pettersson, Nuclear Instruments **4** (1959) 107
38) I. Marklund, B. v. Nooijen and Z. Grabowski, Nuclear Physics **15** (1960) 533
39) S. Hultberg, Nuclear Instruments **10** (1961) 24
40) M. Stobbe, Ann. Physik **7** (1930) 661
41) T. Suter and P. Reyes-Suter, Arkiv f. Fysik, to be published
42) M. Vergnes, Ann. Physique **5** (1960) 11
43) P. Reyes-Suter and T. Suter, to be published
44) E. M. Bernstein and H. W. Lewis, Phys. Rev. **105** (1957) 1524
45) J. de Boer, Helv. Phys. Acta **32** (1959) 377